

Tower shadow excitation of a downwind rotor blade of a turbine with a tubular tower

van der Male, P.; van Schaik, R.; Vergassola, M.; van Dalen, K.N.

DOI

[10.1088/1742-6596/1618/3/032019](https://doi.org/10.1088/1742-6596/1618/3/032019)

Publication date

2020

Document Version

Final published version

Published in

Journal of Physics: Conference Series

Citation (APA)

van der Male, P., van Schaik, R., Vergassola, M., & van Dalen, K. N. (2020). Tower shadow excitation of a downwind rotor blade of a turbine with a tubular tower. *Journal of Physics: Conference Series*, 1618(3), Article 032019. <https://doi.org/10.1088/1742-6596/1618/3/032019>

Important note

To cite this publication, please use the final published version (if applicable). Please check the document version above.

Copyright

Other than for strictly personal use, it is not permitted to download, forward or distribute the text or part of it, without the consent of the author(s) and/or copyright holder(s), unless the work is under an open content license such as Creative Commons.

Takedown policy

Please contact us and provide details if you believe this document breaches copyrights. We will remove access to the work immediately and investigate your claim.

PAPER • OPEN ACCESS

Tower shadow excitation of a downwind rotor blade of a turbine with a tubular tower

To cite this article: P van der Male *et al* 2020 *J. Phys.: Conf. Ser.* **1618** 032019

View the [article online](#) for updates and enhancements.



IOP | ebooks™

Bringing together innovative digital publishing with leading authors from the global scientific community.

Start exploring the collection—download the first chapter of every title for free.

Tower shadow excitation of a downwind rotor blade of a turbine with a tubular tower

P van der Male, R van Schaik, M Vergassola, K N van Dalen

Faculty of Civil Engineering and Geosciences, Delft University of Technology,
Stevinweg 1, 2628 CN Delft, Netherlands
p.vandermale@tudelft.nl

Abstract. The downwind configuration of wind turbines offers benefits regarding the blade-tower clearance, as during operation the blade primarily bends away from the tower. Consequently, the blades can be designed with lower stiffness. For tubular towers, however, a significant deficit of the wind speed in the tower wake occurs, resulting in fatigue-inducing vibrations. For this reason, full-height lattice towers are considered the preferred support structures for wind turbines with a downwind rotor. This work estimates the tower shadow excitation of a downwind rotor blade from a tubular tower. To this end, the blade of a commercial 6 MW downwind turbine is modelled with finite-elements. The tower wake is described on the basis of Madsen's model and for the unsteady aerodynamic interaction Küssner's function is adopted. At below- and above-rated wind conditions, the tower wake-induced vibrations are compared with the response of a blade of an equivalent upwind rotor, considering both the tip deflections and the root moments, the latter on the basis of damage-equivalent moments, to obtain an indication of the expected difference in fatigue damage. The downwind blade experiences vibrations with considerable larger amplitudes, especially in the out-of-plane direction. From the damage-equivalent moments it can be inferred that the blades of the downwind rotor encounter a much faster accumulation of fatigue damage.

1. Introduction

With the increasing rotor dimensions, downwind rotor configurations may become an attractive alternative, compared to the conventional upwind rotor configurations. A downwind rotor is positioned behind the turbine tower, so that the inflow first passes the tower before it reaches the rotor. The main benefit of this concept relates to the blade flexibility, as the wind primarily deforms the blades away from the tower, rendering the design criterion on blade clearance less restrictive [1].

In the wake behind the tower, however, lower mean wind speeds with more turbulence occur. This phenomenon is known as tower shadow. While passing through the tower wake, the blades experience a short deficit in inflow conditions, imposing a dynamic excitation. The consequences of this excitation are twofold. First, the stress variations in the blades and the drive-train induce fatigue, and second, the low-frequency sound waves radiated by the vibrating blades can be perceived as displeasing [2, 3]. To a lesser extent, upwind rotors experience these effects as well, since the wind flow in front of the tower is affected by the presence of the structure too. The tower shadow effect for upwind configurations, however, is smaller than for downwind configurations.

In comparison with tubular towers, the open structure of full-height lattice towers is believed to generate a smaller wake deficit [4, 5]. Especially for bigger turbines and deep water offshore locations, this tower concept provides an appealing solution [6]. The lower aesthetical appreciation, however, makes this tower concept, and subsequently the downwind rotor configuration, inconvenient for



onshore applications. To increase the competitiveness of onshore downwind turbines, the dynamic excitation of the blades by the wake of a tubular tower should be studied further. Once the actual excitation is better understood, the resulting stress variations and sound radiation can be predicted more accurately and novel mitigation strategies, for instance by means of individual pitch control, can be developed.

Previous studies [7, 8] have addressed the loads on a blade of a downwind rotor by solving the Navier-Stokes equations, including a sliding mesh to represent an aerofoil passage. By prescribing the aerofoil motion, the dynamic blade response, including the contribution of the added damping, was not included. Such an estimation by means of CFD would require the coupled modelling of the aerodynamics and the fluid-structure interaction. An overview of the available CFD and FE approaches for the analysis of horizontal axis wind turbines was provided by [9]. The authors concluded that the cost and complexity are still the main obstacles when applying combined CFD and FE approaches for wind turbine analyses, especially when transient conditions are to be accounted for.

A computationally less expensive approach entails the decoupling of the modelling of the wake development behind the tubular tower and the subsequent fluid-structure interaction of the rotating blade. Regarding the former, different textbooks make reference to Powles's method [3, 9], which finds its basis in an experimental study [11] and which is offered by aeroelastic tools such as BLADED. The application of this method for modern wind turbines, however, cannot be justified with the Reynolds numbers for which the experiments were conducted. Other available methods lack a validation with measurements in a representative Reynolds regime [12, 13], or allow for far-wake predictions only [14]. The most applicable models for a decoupled analysis would be Madsen's model [15], which expresses the lateral and axial wake velocities in terms of the drag coefficient of the turbine tower. Madsen's wake model showed good correspondence with the simulated wake-averaged velocities presented by [16]. In this study, the wake behind a tubular tower was modelled by means of a finite-volume discretisation of the incompressible Reynolds-averaged Navier-Stokes equations, for a representative tower diameter and wind speed. It should be noted, however, that Madsen's model does not account for tower-induced turbulence.

The objective of the current study is a quantification of the tower shadow excitation for a downwind rotor behind a tubular tower, using a decoupled modelling approach and Madsen's tower wake formulation. To this end, the blade tip motion and the damage-equivalent root moment of a commercial two-bladed 6 MW downwind turbine are estimated, providing a basis for the further estimation of the induced fatigue and sound radiation. A comparison with the blade response of an equivalent upwind turbine generates insight in the extent of the relative impact of the tower shadow effect for the considered downwind turbine. To describe this upwind wake, use is made of the wake model presented by [10]. This upwind wake model describes a two-dimensional wake in front of a tubular tower, based on the potential flow theory.

The tower shadow responses are estimated for turbulent inflow conditions with mean wind speeds in the below- and above-rated regimes. To model the blade response, use is made of a structural single-blade model [17], which is extended to include torsional motions too. The aerodynamic modelling is based on the relative flow velocities, accounting for the aeroelastic coupling. As a consequence, aerodynamic damping of the blade oscillations is implicitly included. The downwind tower wake imposes a strong spatial non-uniformity in the wind field, which requires an unsteady aerodynamic model [18]. In this respect, use is made of the unsteady lift model on the basis of Küssner's function [19], which allows for a time-domain analysis of incident airflow variations. The adopted unsteady lift model assumes attached flow conditions. As no description of the control system was available, both the rotational speed and the pitch angle are kept constant in the simulations.

2. Blade model and aerodynamic forcing

2.1. Turbine characteristics

For this study, the blade characteristics of the 2B6 turbine are adopted. The rotor diameter is 140.6 m and the hub radius is 2.05 m, leaving a blade length of 68.25 m. The cut-in and cut-out wind speeds are 4 m/s and 25 m/s, respectively and the rated wind speed is approximately 10 m/s. Table 1 presents the rotor speed and pitch angle variations within the operational regime of the wind turbine.

For the analysis of the blade response to tower shadow excitations, the rotational velocity affects the relative inflow velocity and consequently the aerodynamic forcing of the blade. Moreover, the rotational speed is of relevance for the centrifugal stiffening of the blade, affecting the natural frequencies, and the centrifugal forcing. The pitch angle affects the angle of attack of the relative wind speed along the length of the blade, and therefore the aerodynamic loading. The pitch angle also determines the orientation of the blade cross-sections within the rotational plane, as a result of which the flapwise and edgewise contributions to the out-of-plane and the in-plane blade vibrations are affected.

To estimate the blade response to the tower shadow excitation, the operational conditions for both 7 m/s and 16 m/s are considered. These wind speeds correspond to either below- and above-rated conditions. The analysis of the tower shadow excitation assumes a tubular wind turbine tower. With respect to the geometry of this tower, a constant diameter of 4 m is adopted, based on the geometry of the tower of the NREL5 turbine [20], the dimensions of which vary from 3.87 m at the top to 6 m at the bottom. The overhang of the rotor at the nacelle is 8.16 m and the tilt and cone angles of the rotor are 3 degrees and 6 degrees, respectively.

Table 1. Rotational speed and blade pitch angle per wind speed.

Wind speed [m/s]	Rotational speed [rpm]	Blade pitch angle [deg]
5	8.20	1.20
7	10.14	1.20
10	11.80	1.20
12	11.80	1.20
16	11.80	10.98
25	11.80	23.41

2.2. Structural blade model

The aerodynamic excitation of a flexible rotating blade depends non-linearly on the structural motions. To analyze the tower shadow effect on the rotating blade, use is made of a Galerkin decomposition, which requires the definition of mass-normalized modes and corresponding natural frequencies. These dynamic characteristics are obtained from a finite-element model of the rotating blade, which was based on [17]. This work described a model of a rotating wind turbine blade in a rotating reference frame, including centrifugal stiffening, and is extended here with the inclusion of torsional degrees of freedom.

The mass-normalized structural mode shapes of the first six modes of vibration obtained from an eigenanalysis at a wind speed of 12 m/s – with a rotational speed of 11.8 rpm – are presented in Figure 1. Here, it should be noted that the operational state affects the centrifugal stiffening and therefore the dynamic properties of the blade. It can be seen that modes 1, 3 and 5 dictate the out-of-plane motion, whereas modes 2 and 4 mainly relate to motions within the plane of rotation. For modes 4 and 6, a coupling with the torsional motion of the blade can be observed. The first six natural frequencies of the blade, as obtained with the current model, are presented in Table 2, and compared with a similar model developed with the aeroelastic software BLADED 4.6. With the exception of the second edgewise mode, the differences are considered to be small. To model the dynamic response of the blade, a structural damping of 0.5% of the critical damping is adopted for all modes, which is in correspondence with [20].

2.3. Modelling the aerodynamic excitation

The aerodynamic modelling is based on the relative flow velocities, resulting from the inflow velocity minus the structural motions. As a consequence, aerodynamic damping of the blade oscillations is implicitly accounted for. Moreover, since the aerodynamic excitation depends non-linearly on the flow velocity, the lift and drag forces now relate non-linearly to the structural motion. On the other hand, the effect of the structural motions on the inflow conditions is neglected. Hence, the inflow conditions and the blade vibrations are only coupled in a one-sided manner.

To model the excitation from the tower passing, the unsteady lift coefficient is determined on the basis of Küssner's function, which allows for a time-domain analysis of incident airflow variations. For this work, the double time-lag approximation of Küssner's function in accordance with [19] is applied. On the other hand, attached-flow conditions are assumed. In principle, the angle of attack along the blade is small, and only towards the root flow separation occurs. While crossing the tower wake, a change in inflow conditions occurs and the equilibrium of the circulatory flow around the blade is briefly disrupted. For this short disruption, an overshoot of the linear lift force can be assumed.

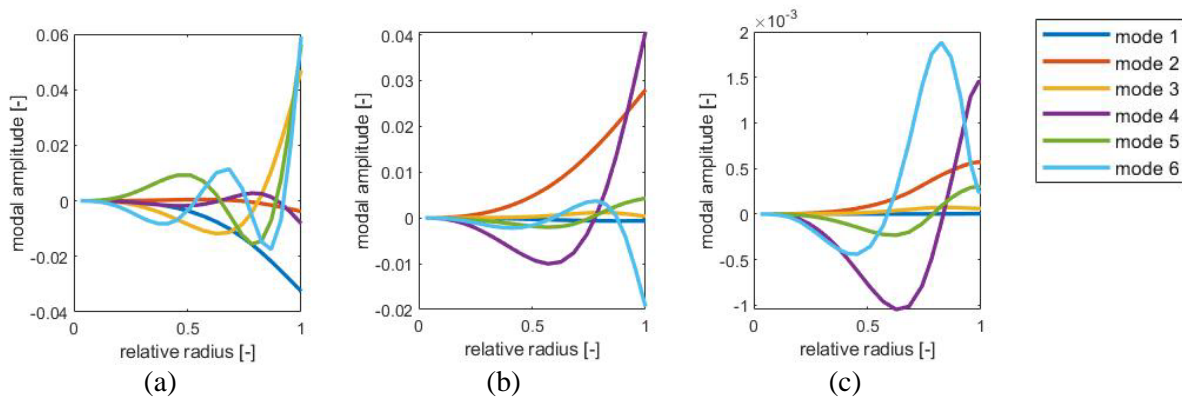


Figure 1. Representation of the first six mode shapes for the operational conditions at an upstream inflow velocity of 12 m/s, with (a) the mode shape components in the out-of-plane direction, (b) the mode shape components in the in-plane direction, and (c) the torsional mode shape components.

Table 2. Natural frequencies of the first six modes as obtained from the current model and BLADED.

mode	current model	BLADED
1 st flapwise	0.69 Hz	0.64 Hz
1 st edgewise	1.14 Hz	1.10 Hz
2 nd flapwise	1.93 Hz	1.90 Hz
2 nd edgewise	3.53 Hz	4.48 Hz
3 rd flapwise	4.12 Hz	4.14 Hz
3 rd edgewise	7.07 Hz	6.96 Hz

3. Downwind and upwind wake modelling

3.1. Configuration and scenarios

Figure 2 indicates the orientation of the rotating blade behind the turbine tower, distinguishing inflow conditions of 7 m/s and 16 m/s, respectively (Figure 2(a) and (b)). First, the undeformed orientations are illustrated, which are defined by the overhang at the hub and the tilt and the cone angles. Subsequently, the deformed shapes are depicted, which are used to define the inflow conditions in the wake behind the tower. These shapes are obtained from the aerodynamic loading corresponding to the mean inflow velocity, and the counteracting centrifugal force from the rotation of the rotor.

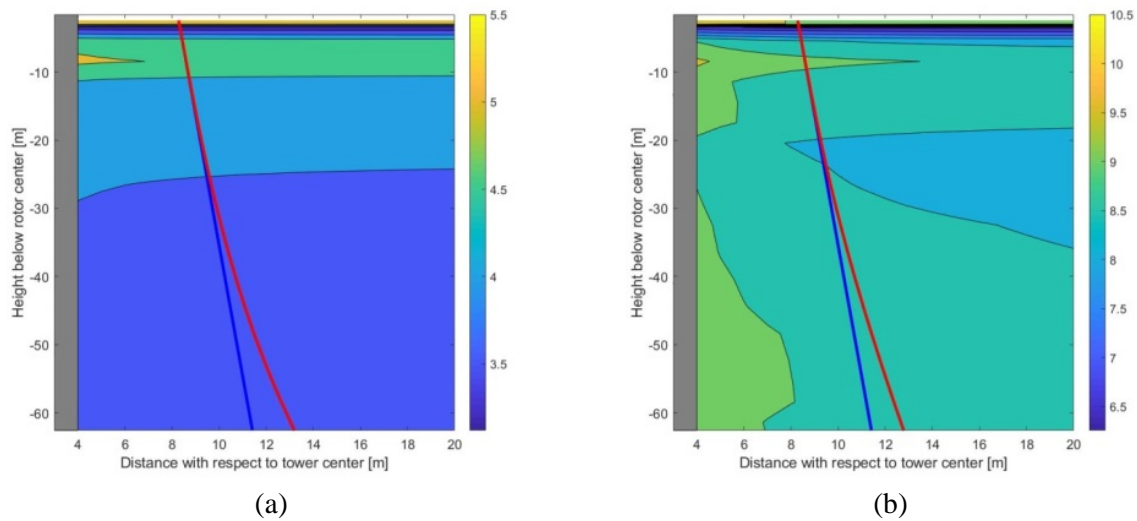


Figure 2. Longitudinal cross-sections of the wake behind the centre of the tower (indicated in grey), including an indication of the unloaded blade positioning (in blue) and the statically loaded blade position (in red), for upstream wind velocities of (a) 7 m/s, (b) 16 m/s. The colouring indicates the different mean flow velocities in the wake, as obtained with Madsen's model.

3.2. Wake developments

For the downwind tower shadow wake, Madsen's model is adopted, as described in [16]. This approach was shown to give similar results as CFD simulations, which accounted for the correct flow regime. Madsen's model describes the velocities in lateral and longitudinal directions of a uniform flow around a cylindrical tower. As the flow is defined in 2D, the model implicitly assumes an infinitely long tower. The description of the flow can be based on the drag coefficient of the tower, which is in the range of 0.3 to 0.7 for Reynolds numbers between 10^6 to $3.5 \cdot 10^6$ and 0.7 for higher Reynolds numbers.

Figure 2 presents the wake developments in the longitudinal direction at the centre of the tower for the adopted mean inflow conditions. In defining the wakes, the equilibrium wake at the rotor plane is accounted for, as a consequence of which the varying flow velocities in the vertical direction can be observed. With the implementation of the equilibrium wake, the inflow conditions at the tower are modelled more precisely, as these can vary significantly from the upstream inflow conditions. On the other hand, with the varying flow conditions along the length of the tower the validity of the 2D Madsen's model is violated to a certain extent.

It can be seen that for the low inflow velocities, in this case 7 m/s, the longitudinal flow within the wake does not differ much, implying that the blade clearance is of not much effect on the tower shadow excitation. For higher inflow velocities, the deficit even increases for larger distances behind the tower. It should be noted that Madsen's model does not account for turbulence within the tower shadow wake. When considering the wake conditions in relation to the deflected blade, as it enters the wake, it can be seen that the inflow conditions at the blade will not change much, justifying an uncoupled analysis of the inflow conditions and the blade vibrations.

To describe the upwind wake, for an equivalent upwind turbine, use is made of the wake model presented in [10]. This upwind wake model describes a two-dimensional wake in front of a tubular tower, based on the potential flow theory. The potential due to the tower shadow is represented by a closely spaced source and sink in a unidirectional flow field. From the potential, the disturbed flow field in front of the tower can be calculated.

3.3. Rotating blade excitations

The blade response to the tower shadow excitation is simulated for turbulent inflow conditions. To this end, turbulent time series have been generated in correspondence with IEC-3 (class A) with mean wind speeds of 7 m/s and 16 m/s, respectively. To investigate the tower shadow effect, either the Madsen wake profiles or the upwind tower shadow wake profiles based on potential flow analysis have been superimposed to the turbulent wind fields.

For the analysis, turbulent wind files with a total length of 600 s have been generated. Figure 3 and Figure 4 provide a 10-second time window of the turbulent inflow conditions experienced by the rotating blade. Figure 3(a) presents the wind velocity along the length of the blade of the downwind rotor for a mean wind speed of 7 m/s and Figure 3(b) the wind velocity of the corresponding upwind rotor. The instances at which the blade passes the centre line of the tower are indicated in the figures. The differences between the wind speeds of both figures result from the different configuration of the rotor. A much clearer difference between the velocity profiles for the downwind and the upwind rotor is observed for the turbulence inflow with a mean wind speed of 16 m/s. Figure 4(a) presents a time window of the wind velocity for the blade of the downwind rotor and Figure 4(b) of the upwind rotor. At the indicated instances, the deficit in the wind velocity along the length of the blade is visible, especially for the downwind configuration.

Figure 5 presents the power spectral densities of the inflow conditions at the blade tip, for mean wind speeds of 7 m/s and 16 m/s, Figure 5(a) and (b), respectively. The presented power spectral densities represent either a turbulent inflow with downwind wake or upwind wake disturbances, corresponding to a downwind or upwind rotor configuration. For comparison reasons, the power spectral densities of the undisturbed flow (without tower wake), are presented as well. The peaks in the spectra correspond with the rotor harmonics, i.e., multiples of the frequency of blade revolutions. It can be seen that the size of the peaks is larger in case of downwind wake disturbances, especially for the mean wind speed of 16 m/s. On the other hand, the difference between the undisturbed wind field and the wind field with upwind wake disturbances is small. It can therefore be expected that the upwind wakes will not affect the blade motions much (compared to the motions in the undisturbed wind field), whereas the downwind wakes will affect the blade motions.

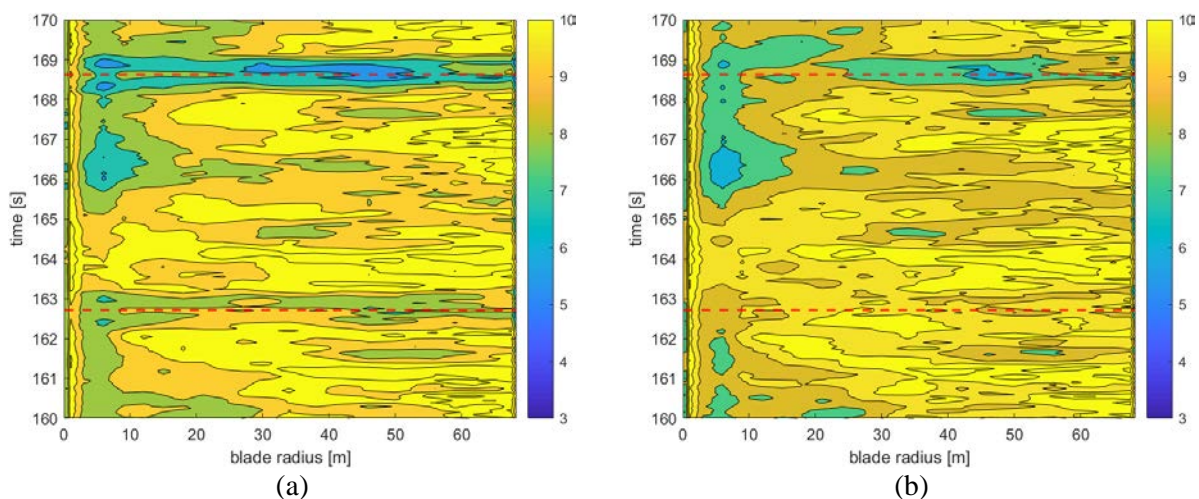


Figure 3. Ten-second time window of the turbulent inflow with a mean wind speed of 7 m/s along the blade length, for (a) an downwind configuration, and (b) an upwind configuration. The colouring indicates the flow velocity and the red dashed lines indicate the time instances of the blade passing the centre line of the tower.

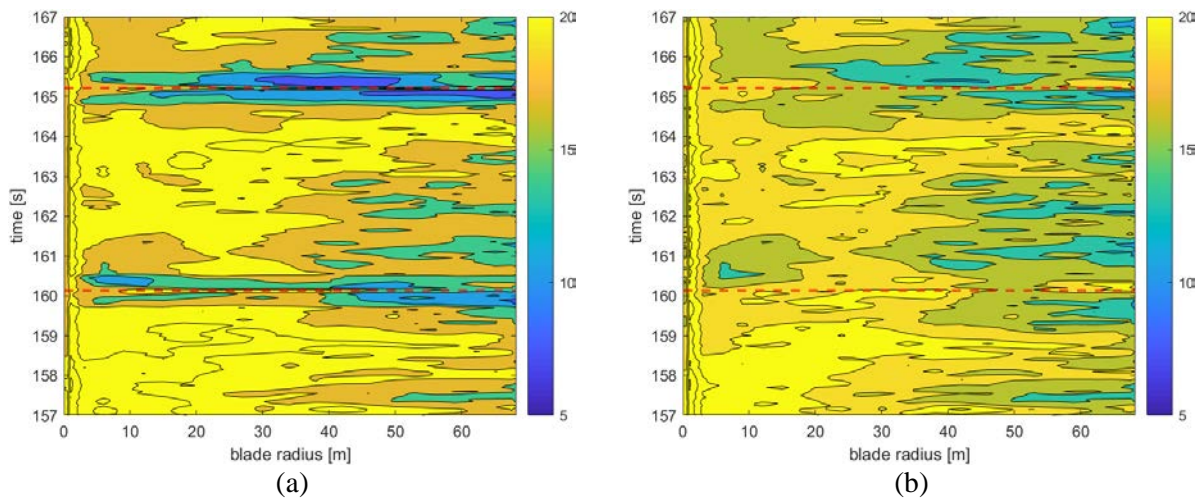


Figure 4. Ten-second time window of the turbulent inflow with a mean wind speed of 16 m/s along the blade length, for (a) an downwind configuration, and (b) an upwind configuration. The colouring indicates the flow velocity and the red dashed lines indicate the time instances of the blade passing the centre line of the tower.

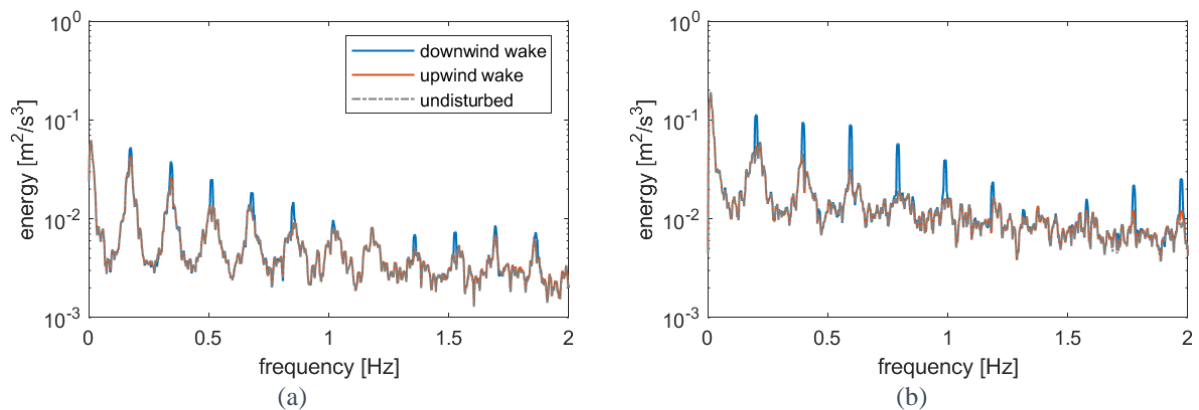


Figure 5. Power spectral density of the inflow velocity at the blade tip for downwind and upwind configurations, compared with the undisturbed inflow, for a mean wind speed of (a) 7 m/s, and (b) 16 m/s.

4. Response Estimation

4.1. Wake-excited blade vibrations

For the operational conditions defined in Section 2.1, and the downwind and upwind wake excitations as presented in Section 3.3, 50-second time windows of the out-of-plane and in-plane blade tip motions are given in Figure 6 and Figure 7, respectively. For a mean wind speed of 7 m/s, the differences in the blade tip deflections between the downwind and the upwind configurations are small, concerning both the in-plane and out-of-plane oscillations, Figure 6(a) and (b), respectively. Figure 7(a) and (b) present the oscillations resulting for the mean wind speed of 16 m/s. For this case, the amplitudes of the oscillations are larger than for the 7 m/s mean wind speed. Moreover, the difference between the downwind and upwind configurations is clearly visible.

After removing the first 100 s of the response simulations, thereby excluding the transient response resulting from the initial conditions, the power spectral densities of both the in-plane and the out-of-

plane blade tip deflections have been determined for both inflow conditions. These power spectral densities are presented in Figure 8 and Figure 9. The out-of-plane motions show distinguished peaks at the multiple of the rotor frequency. Due to the large amount of aerodynamic damping, no peak at the first natural frequency, which relates to the first out-of-plane mode of vibrations, can be discerned. The in-plane motions, Figure 9 do contain an emphasized peak around 1.10 Hz, which corresponds with the second mode of vibration, indicating that the motion is governed by the first edgewise bending mode. When comparing the blade tip response for the downwind and upwind configurations, it becomes clear that the former results into larger peaks at the multiples of the rotor frequency, especially for the mean inflow velocity of 16 m/s. The difference between the peaks at the second natural frequency, Figure 9(a) and (b), is very small.

The maximum amplitudes of the tip oscillations, with respect to the mean deformation, are presented in Table 3. In this respect, the maximum out-of-plane oscillation is of particular relevance, as it directly relates to the required blade clearance. The simulation based on a mean wind speed of 16 m/s results in a maximum blade tip deflection towards the tower of 5.8 m, with respect to the mean deflection, which is 22% higher than the maximum amplitude for an equivalent upwind configuration. When comparing the maximum deflections to towards the tower only, the difference is even 34%. The relative difference between the out-of-plane deflections for 7 m/s is substantial as well, whereas the difference between the in-plane deflections is less considerable.

Since the model accounted for both inflow turbulence and tower shadow excitation, the maximum blade tip deflections express the most unfavourable combination of both during the performed simulations. The standard deviations of the blade tip oscillations, presented in Table 4, express the overall variability of the motions. Regarding the out-of-plane motion, the downwind configuration results in a considerable larger variation than the upwind configuration. For the mean inflow velocity of 7 m/s the difference between the standard deviations of the in-plane blade tip motions is small, as these motions are mainly induced by the inflow turbulence. For 16 m/s, the contribution of the downwind tower wake is significant, resulting in a substantial difference between the standard deviations of the downwind and upwind configurations.

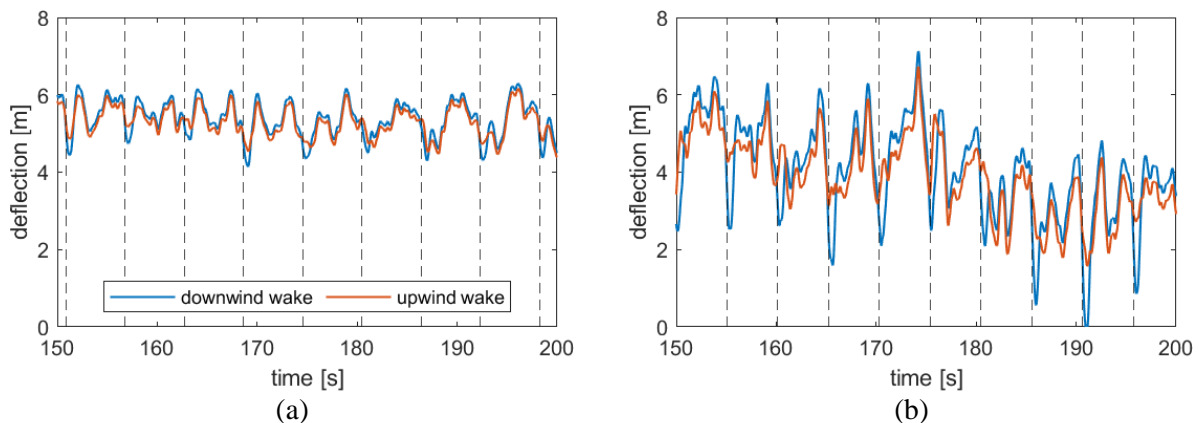


Figure 6. Out-of-plane blade motions, relative to the mean deflection, for turbulent inflow conditions with a mean wind velocity of (a) 7 m/s, and (b) 16 m/s. The dashed lines indicate the instances that the blade passes the centre line of the tower.

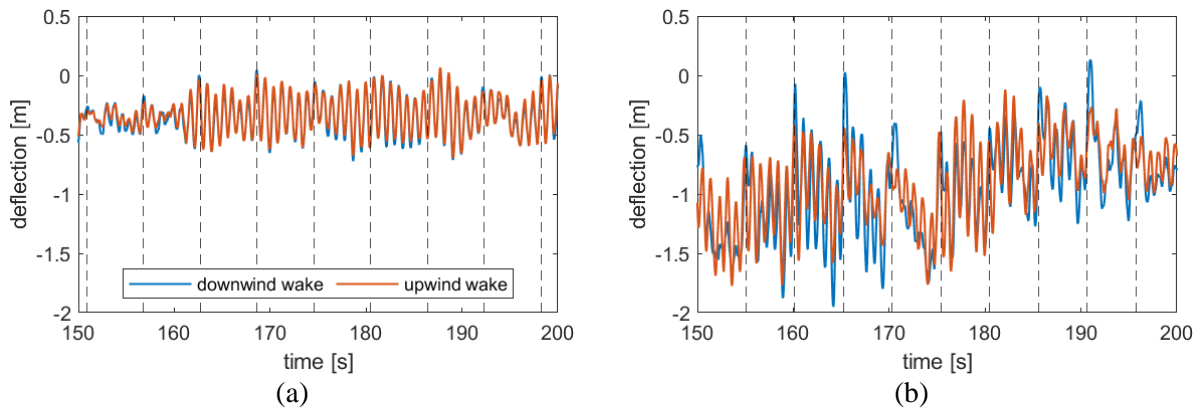


Figure 7. In-plane blade motion, for mean upstream wind velocities of (a) 7 m/s, and (b) 16 m/s. The dashed lines indicate the instances that the blade passes the centre line of the tower.

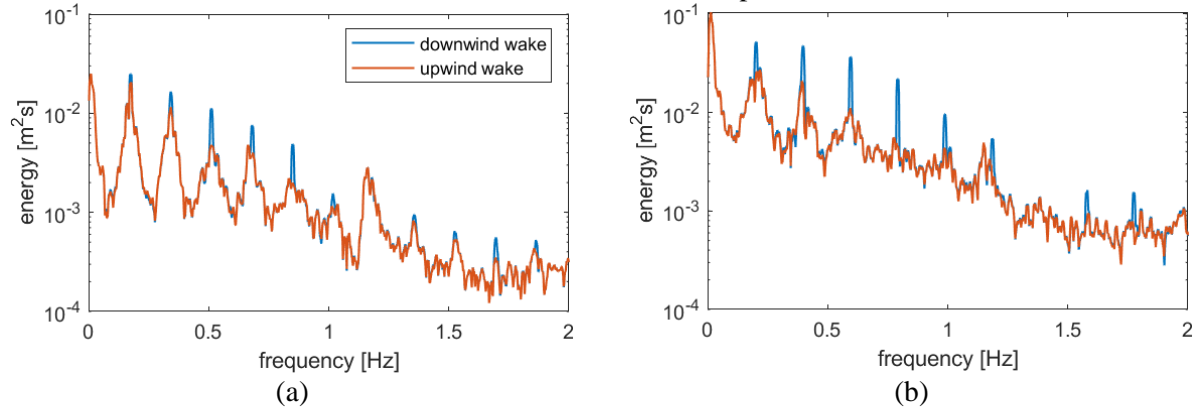


Figure 8. Power spectral densities of the out-of-plane blade tip motions, for turbulent inflow conditions with a mean wind velocity of (a) 7 m/s, and (b) 16 m/s.

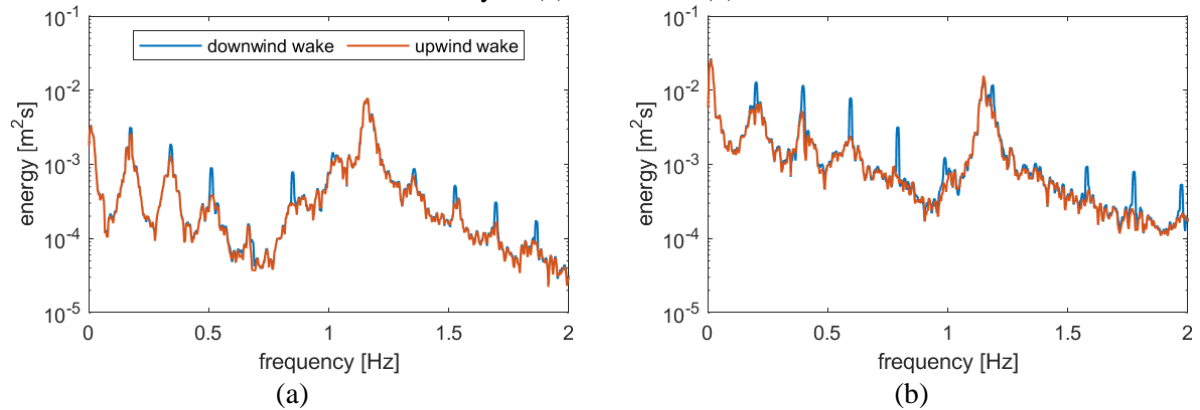


Figure 9. Power spectral densities of the in-plane blade tip motions, for turbulent inflow conditions with a mean wind velocity of (a) 7 m/s, and (b) 16 m/s.

Table 3. Maximum amplitude of out-of-plane and in-plane blade tip oscillations.

inflow velocity	out-of-plane motion			in-plane motion		
	downwind	Upwind	difference	downwind	upwind	difference
7 m/s	1.996 m	1.611 m	23.9%	0.571 m	0.562 m	1.72%
16 m/s	5.817 m	4.763 m	22.1%	1.753 m	1.642 m	6.71%

Table 4. Standard deviations of the out-of-plane and in-plane blade deflections.

inflow velocity	out-of-plane motion			in-plane motion		
	downwind	Upwind	difference	downwind	upwind	difference
7 m/s	0.544 m	0.494	9.99 %	0.157 m	0.154 m	1.87 %
16 m/s	1.688 m	1.495	12.9 %	0.495 m	0.444 m	11.5 %

Root moment comparison

In addition to the comparison of the blade tip oscillations, the root moment variations as a result of the downwind and upwind wake excitations are compared. To do so, the root moments are calculated from the curvature of the blade at the root, multiplied with the blade root bending stiffness. From the time signals of the resulting root moments, the damage-equivalent blade root moments have been determined, in accordance with [20]. As the blade root consists of both steel and composite components, the damage-equivalent moments are determined for inverse S-N slopes of 4 and 9, respectively. Subsequently, the damage-equivalent moments are expressed in terms of 1 Hz cycles, resulting in values which are independent of the governing natural frequency of the blade.

The 1-Hz damage-equivalent blade root moments are presented in Table 5 and Table 6, for either steel or composite material. The tables distinguish the out-of-plane bending and in-plane bending for both rotor configurations and considered mean wind speeds. The absolute values of the damage-equivalent moments depend on the inverse S-N slope, whereas the relative difference between the downwind and upwind configurations does not (the relative difference can directly be obtained from the standard deviations of the moment time series). For both materials, the largest damage-equivalent moments are obtained for the out-of-plane bending.

When comparing the damage-equivalent moments from the downwind and upwind wakes, it becomes immediately clear that the differences for the mean inflow velocity of 7 m/s are small (< 5%), whereas for the simulations with a mean wind speed of 16 m/s a substantial difference is obtained (ca. 13%). This leads to the conclusion that, for equal blade designs, the fatigue damage at the blade root will accumulate at a significantly faster rate for a downwind configurations than for upwind configuration. This effect is stronger for higher wind speeds, as these result in a larger tower wake deficit.

Table 5. 1-Hz damage-equivalent blade root moments for steel components.

inflow velocity	out-of-plane bending			in-plane bending		
	Downwind	Upwind	difference	downwind	upwind	difference
7 m/s	13.9 kNm	13.9 kNm	0.64 %	5.99 kNm	5.85 kNm	2.38 %
16 m/s	27.9 kNm	24.7 kNm	13.2 %	17.2 kNm	15.2 kNm	13.3 %

Table 6. 1-Hz damage-equivalent blade root moments for composite components.

inflow velocity	out-of-plane bending			in-plane bending		
	Downwind	Upwind	difference	downwind	upwind	difference
7 m/s	19.4 kNm	19.2 kNm	0.64 %	7.71 kNm	7.53 kNm	2.38 %
16 m/s	38.8 kNm	34.3 kNm	13.2 %	22.2 kNm	19.6 kNm	13.3 %

5. Conclusions and recommendations

For this study, a comparison of the wake effect for a downwind turbine and an equivalent upwind turbine was presented. The downwind wake was described on the basis of Madsen's model, accounting only for wake-averaged velocity deficits. No wake turbulence was accounted for. The description of the upwind wake was based on the potential flow theory. Concerning the inflow, turbulent time series were generated for wind class IEC-3 (class A) with mean wind speeds of 7 m/s and 16 m/s, corresponding to the below and above-rated operational regime. The downwind wake was shown to affect the inflow conditions considerably, whereas for the upwind wake only a small influence could be discerned.

A dynamic finite-element model of the blade of a commercial 6MW turbine was developed, including the centrifugal stiffening effect. The aerodynamic modelling included one-sided aeroelastic coupling, implying that aerodynamic damping of the blade oscillations is implicitly accounted for. Concerning the aerodynamic excitation, unsteady aerodynamic lift was modelled on the basis of Küssner's function, to account for the spatial variation in the inflow conditions. Regarding the comparison, blade tip motions and the root moments were compared. For both configurations, the dynamic response was shown to be governed by the second bending mode, inducing edgewise vibrations, as the aerodynamic damping of this mode is much smaller than the damping of the first bending mode.

The simulation based on a mean wind speed of 16 m/s results in a maximum amplitude of blade tip oscillation of 5.8 m, with respect to the mean deflection, which is 22% higher than the maximum amplitude of oscillation for an equivalent upwind configuration. The maximum out-of-plane deflection is of particular relevance for design, as it relates directly to the required blade clearance, and when the maximum deflections towards the tower are compared, the difference is even 34%. The relative difference between the out-of-plane amplitudes for 7 m/s is substantial as well, whereas the difference between the in-plane deflections is less considerable. The standard deviation of the out-of-plane motion is considerably larger for the downwind configuration too (10 to 13%). For the above-rated simulation, also the downwind in-plane motion showed a substantial larger variability.

In addition to the out-of-plane and in-plane blade tip motions, the resulting root moments from the wake excitations were compared. To do so, 1-Hz damage-equivalent moments were presented for the different operational conditions. In this respect, both steel and composite components were distinguished. Comparing the damage-equivalent moments of the downwind and upwind wake excitations, it was obviously shown that the downwind wake induces a fatigue damage accumulation at a faster rate (up to 13.3%) than the upwind configuration, particularly for the considered above-rated operational conditions, implying that the fatigue capacity of the downwind blade must be considerably larger.

Regarding the validity of the applied tower wake model, it should be noted that Madsen's model only provides a two-dimensional description of the wake and was obtained from CFD simulations of a cylinder in a uniform flow. As a consequence, the model does not account for three-dimensional effects, resulting from non-uniform flows, non-prismatic and/or discontinuous towers, all of which apply for the fluid-structure interaction of a wind turbine tower. Moreover, the model does not provide a description of the turbulence in the wake, whereas the CFD simulations indicated significant turbulence levels. Further research would require a better description of the wake conditions behind a tubular tower of a wind turbine.

The aerodynamic forcing was described for attached flow conditions. It should be validated to what extent dynamic stall needs to be accounted for. The aerodynamic forcing was described on the indicial response theory, where Küssner's function was adopted to describe the establishment of the aerodynamic equilibrium. In determining the aerodynamic forcing, the wake inflow conditions were not coupled to the motion of the blades.

In terms of the predicted response, larger blade tip deflections were shown for the downwind wake, compared to the analyses with an upwind wake. Also the root moments consisted of higher moment ranges for the downwind wake excitations. It could be investigated to what extent an individual pitch control could mitigate the excitations of the downwind wake. This does not just concern the mitigation of the wake excitation itself – pre-and post-pitching could reduce the total variation in the angle of attack during the tower passing – but perhaps even more the mitigation of the transient response, by trying to increase the level of aerodynamic damping.

A further study could aim to couple the wake and the blade response, for instance by means of a CFD analysis. Such an analysis would involve the modelling of a rotating flexible blade and requires a basic understanding of the expected blade response. The current work can provide this understanding, and can therefore serve as a basis for more advanced CFD studies.

Acknowledgements

The presented study was part of the EX2BE project, funded by the Netherlands Enterprise Agency, with the project partners 2-B Energy and TRES4.

References

- [1] Koh J H and Ng E Y K 2016 Downwind offshore wind turbines: opportunities, trends and technical challenges. *Ren. and Sus. En. Rev.* **54** p 797–8
- [2] Wagner S, Bareiss R and Guidati G 1996 *Wind turbine noise* (Berlin: Springer)
- [3] Jamieson P 2018 *Innovation in wind turbine design* (London: Wiley)
- [4] Reiso M and Moe G 2010 Blade response on offshore bottom fixed wind turbines with downwind rotors *Proc. ASME 29th Int. Conf. Ocean, Offshore and Arctic Eng.* (Shanghai) p 499–4
- [5] Van Solingen E, Beerens J, Mulders S P, De Breuker R and Van Wingerden J W 2016 Control design for a two-bladed downwind teeterless damped free-yaw wind turbine *Mechatronics* **36** p 77–96
- [6] Vergassola M, Cabboi A and Van der Male P 2020 Offshore support structure concepts comparison for a 14 MW two-bladed downwind wind turbine, *Journal of Physics: Conference Series* IOP Publishing (accepted for publication)
- [7] Janajreh I, Qudaih R, Talab I and Ghenai C 2010 Aerodynamic flow simulation of wind turbine: downwind versus upwind configuration *Energy Conversion and Man.* **51**(8) p 1656–63
- [8] Zahle F, Madsen H A and Sørensen N N 2009 Evaluation of tower shadow effects on various wind turbine concepts 2007 *In Research in Aeroelasticity EFP-2007-II* Danmarks Tekniske Universitet, Risø Nationallaboratoriet for Bæredygtig Energi p 11–29
- [9] O'Brien J M, Young T M, O'Mahoney D C and Griffin P C 2017 Horizontal axis wind turbine research: a review of commercial CFD, FE codes and experimental practices *Progr. in Aeros. Sci.* **9** p 1–24
- [10] Burton T, Jenkins N, Sharpe D and Bossanyi 2011 *Wind energy handbook*, 2nd Ed. (West Sussex, UK: Wiley)
- [11] Powles S R J 1983 The effects of tower shadow on the dynamics of a horizontal-axis wind turbine *Wind Eng.* **7**(1) p 26–42
- [12] Wang T and Coton F N 2001 A high resolution tower shadow model for downwind wind turbines *J. of Wind Eng. and Ind. Aerod.* **89** p 873–92
- [13] Munduate X, Coton F N and Galbraith R A M 2004 An investigation of the aerodynamic response of a wind turbine blade to tower shadow *J. of Solar Energy Eng.* **126**(4) p 1034–40
- [14] Schlichting H and Gersten K 2017 *Boundary-layer theory* (Berlin: Springer)
- [15] Madsen H A 1982 *Actuator cylinder – a flow model for vertical axis wind turbines* Aalborg University Centre
- [16] Madsen H A, Johansen J, Sørensen N, Larsen G and Hansen M 2007 Simulation of low frequency noise from a downwind wind turbine rotor. *In 45th AIAA Aerospace Sciences Meeting and Exhibit* (Reno, Nevada) AIAA2007– 623
- [17] Van der Male P, Van Dalen K N and Metrikine A V 2016 The effect of the nonlinear velocity and history dependencies of the aerodynamic force on the dynamic response of a rotating wind turbine blade *J. of Sound and Vib.* **383** p 191–9
- [18] Leishman J G 2002 Challenges in modelling the unsteady aerodynamics of wind turbines *Wind Energy: An International Journal for Progress and Applications in Wind Power Conversion Technology* **5**(2-3) p 85–132.
- [19] Sears W R and Sparks B O 1941 On the reaction of an elastic wing to vertical gusts *J. of the Aeron. Sci.* **8**(2), p 64–7
- [20] Jonkman J, Butterfield S, Musial W and Scott G 2009 Definition of a 5-MW reference wind turbine for offshore system development NREL/TP-500-38060 NREL Lab, Golden (US)
- [21] Seidel, M 2014 Wave induced fatigue loads: Insights from frequency domain calculations *Stahlbau* **83**(8) p 535–41